

RESEARCH ARTICLE

Utilizing Targeted Mass Spectrometry to Demonstrate Asf1-Dependent Increases in Residue Specificity for Rtt109-Vps75 Mediated Histone Acetylation

Yin-Ming Kuo¹, Ryan A. Henry¹, Liangqun Huang², Xu Chen², Laurie A. Stargell², Andrew J. Andrews^{1*}

1 Department of Cancer Biology, Fox Chase Cancer Center, Philadelphia, Pennsylvania, United States of America, **2** Department of Biochemistry and Molecular Biology, Colorado State University, Fort Collins, Colorado, United States of America

* Andrew.Andrews@fccc.edu



OPEN ACCESS

Citation: Kuo Y-M, Henry RA, Huang L, Chen X, Stargell LA, Andrews AJ (2015) Utilizing Targeted Mass Spectrometry to Demonstrate Asf1-Dependent Increases in Residue Specificity for Rtt109-Vps75 Mediated Histone Acetylation. PLoS ONE 10(3): e0118516. doi:10.1371/journal.pone.0118516

Academic Editor: Axel Imhof, Ludwig-Maximilians-Universität München, GERMANY

Received: July 16, 2014

Accepted: January 17, 2015

Published: March 17, 2015

Copyright: © 2015 Kuo et al. This is an open access article distributed under the terms of the [Creative Commons Attribution License](https://creativecommons.org/licenses/by/4.0/), which permits unrestricted use, distribution, and reproduction in any medium, provided the original author and source are credited.

Data Availability Statement: All relevant data are within the paper.

Funding: Research reported in this publication was supported by the W. W. Smith Charitable Trust, the Pennsylvania Department of Health, and the National Institute of General Medical Sciences of the National Institutes of Health under Award Number R01 GM102503 to AJA and GM088409 to LAS. The content is solely the responsibility of the authors and does not necessarily represent the official views of the funders. The funders had no role in study design,

Abstract

In *Saccharomyces cerevisiae*, Rtt109, a lysine acetyltransferase (KAT), associates with a histone chaperone, either Vps75 or Asf1. It has been proposed that these chaperones alter the selectivity of Rtt109 or which residues it preferentially acetylates. In the present study, we utilized a label-free quantitative mass spectrometry-based method to determine the steady-state kinetic parameters of acetylation catalyzed by Rtt109-Vps75 on H3 monomer, H3/H4 tetramer, and H3/H4-Asf1 complex. These results show that among these histone conformations, only H3K9 and H3K23 are significantly acetylated under steady-state conditions and that Asf1 promotes H3/H4 acetylation by Rtt109-Vps75. Asf1 equally increases the Rtt109-Vps75 specificity for both of these residues with a maximum stoichiometry of 1:1 (Asf1 to H3/H4), but does not alter the selectivity between these two residues. These data suggest that the H3/H4-Asf1 complex is a substrate for Rtt109-Vps75 without altering selectivity between residues. The deletion of either Rtt109 or Asf1 *in vivo* results in the same reduction of H3K9 acetylation, suggesting that Asf1 is required for efficient H3K9 acetylation both *in vitro* and *in vivo*. Furthermore, we found that the acetylation preference of Rtt109-Vps75 could be directed to H3K56 when those histones already possess modifications, such as those found on histones purified from chicken erythrocytes. Taken together, Vps75 and Asf1 both enhance Rtt109 acetylation for H3/H4, although via different mechanisms, but have little impact on the residue selectivity. Importantly, these results provide evidence that histone chaperones can work together via interactions with either the enzyme or the substrate to more efficiently acetylate histones.

data collection and analysis, decision to publish, or preparation of the manuscript.

Competing Interests: The authors have declared that no competing interests exist.

Introduction

Rtt109 (KAT11), a fungal-specific lysine acetyltransferase (KAT) that shares structural homology to mammalian p300/CBP [1], was first identified along with Asf1 for its critical role in the acetylation of H3K56 [2]. In addition to H3K56 acetylation, Rtt109 catalyzes the acetylation of several other residues on histone H3 and H4 [3–5]. H3K56 acetylation is unique because it occurs in the globular domain of the histone, suggesting this histone acetylation mark is also directly related to DNA accessibility and transcriptional activation [6–9]. Consistent with this, Rtt109 has been shown to be important for cell survival after exposure to a variety of genotoxic agents [10, 11]. The acetylation of H3K56 requires the histone chaperone Asf1, and the loss of Asf1 will result in a complete loss of K56 acetylation [4].

In general, histone chaperone proteins are highly acidic proteins that directly bind to histones, and guide assembly and disassembly of nucleosomes [12, 13]. Rtt109 has been reported to be activated by two different histone chaperones: Vps75 and Asf1 [14–17]. Rtt109 activation by Vps75 is via direct complexation [4, 18, 19], but it is not clear how Asf1 activates Rtt109. One possible mechanism is via the ability of Asf1 to selectively bind histone H3/H4 [20] and/or split the tetramer (H3/H4)₂ into the dimer 2(H3/H4), thus increasing the available H3/H4 by 2-fold [21, 22].

Rtt109-chaperone complex can acetylate multiple lysines on a single histone, and it has been suggested that Asf1 can alter the selectivity of the residues acetylated [3–5]. The ability of Rtt109 to acetylate multiple residues on a single complex presents problems in understanding its specificity. To fill this gap, we utilize a novel label-free mass spectrometry-based technique that can detect individual lysine acetylation on histone H3 and H4 simultaneously [23, 24]. We have previously used this assay to investigate the differences in specificity and selectivity between CBP and p300 [24] as well as to characterize the specificity of Gcn5 [23].

Specificity refers to the ability of an enzyme to acetylate a specific residue, whereas selectivity pertains to the ability of an enzyme to acetylate one residue relative to another. It has been reported that Rtt109-Vps75 specifically acetylates H3K9 and H3K23, whereas Rtt109-Asf1 is reported to favor the acetylation of H3K56 *in vitro* [5]. Additionally, Rtt109-Asf1 suppresses acetylation at other sites on H3 and H3/H4, compared to Rtt109-Vps75, thereby altering the selectivity [5]. Understanding how these chaperones differentially regulate Rtt109 is therefore important for determining how KAT activity is controlled in the cell.

In this paper, we investigated the specificity and selectivity of acetylation by Rtt109-Vps75 and the influence of Asf1 on this specificity/selectivity. In addition, we determined how specificity changes when transitioning from a substrate of H3 to H3/H4 tetramer, in the presence or absence of Asf1. Here we demonstrated that under steady-state conditions, Rtt109-Vps75 complex primarily targets H3K9 and H3K23, both in the context of the H3/H4 tetramer and on H3 alone. Histone H3 alone was the preferred substrate of Rtt109-Vps75, and demonstrated a higher selectivity for H3K9 over H3K23. The formation of H3/H4 tetramer lowered the specificity of Rtt109-Vps75 and caused the loss of selectivity between K9 and K23. The conversion of H3/H4 tetramer to H3/H4-Asf1 substrate led to an increase in specificity [14, 25], but, interestingly, did not change the selectivity. These results provide important insight into how histone acetylation by Rtt109 is regulated, as well as the factors that influence Rtt109-Vps75 specificity/selectivity.

Materials and Methods

Reagents

All chemicals were purchased from Sigma-Aldrich (St. Louis, MO) or Fisher (Pittsburgh, PA) and were either the highest commercial grade or LC/MS grade. Ultrapure water was generated

from a Millipore Direct-Q 5 ultrapure water system (Bedford, MA). Acetyl-CoA was obtained from Sigma-Aldrich.

Protein preparation and purification

Recombinant *Xenopus* and yeast histones H3 and H4 were purified and provided by the Protein Purification Core at Colorado State University. Histone H3/H4 refolding/tetramerization was done using previously reported methods [26, 27]. Native histone H3/H4 tetramer was purified from chicken erythrocytes and provided by Dr. Studitsky's Lab (Fox Chase Cancer Center, Philadelphia, PA). Single-site acetylated recombinant *Xenopus* H3/H4 tetramers (H3K9ac/H4 and H3K23ac/H4) were provided by Dr. Fierke's Lab (University of Michigan, Ann Arbor, MI). Asf1 and Rtt109-Vps75 complex were expressed and purified following previously described procedures [3, 28, 29]. All purified protein and histone concentrations were determined by UV absorbance and calculated from the extinction coefficients [30–32]. The H3/H4-Asf1 complex was prepared by mixing H3/H4 and Asf1 to the designated molar ratios and then pre-incubating at room temperature for 30 minutes.

KAT assays

Steady-state ($E \ll S$) assays for recombinant *Xenopus* H3, H3/H4, and H3/H4-Asf1 were performed under identical buffer conditions (100 mM ammonium bicarbonate and 50 mM HEPES buffer (pH 7.8)) at 37°C. The assays contained 0.02 to 0.5 μM Rtt109-Vps75 (varied with substrate concentration) and either 0.3–40 μM H3, H3/H4, or H3/H4-Asf1 with saturating acetyl-CoA, or 0.5–500 μM acetyl-CoA with saturating histone. In addition, nonenzymatic experiments were conducted under the aforementioned buffer conditions in the absence of Rtt109-Vps75, with either 2.5 μM H3 or 2.5 μM H3/H4 and 200–500 μM acetyl-CoA. We also carried out a time course study (triplicates) to understand the site-specific details of Rtt109-Vps75 acetylation on recombinant *Xenopus* H3/H4. The experimental conditions were 2 μM H3/H4, 200 μM acetyl-CoA, and 5 μM Rtt109-Vps75 at 37°C. For the acetylation assay comparing various histones (recombinant yeast and *Xenopus* histones and native chicken histones from erythrocytes), 15 μM H3/H4, 200 μM acetyl-CoA, and 0.43 μM Rtt109-Vps75 were added and incubated at 37°C for 1 h. These two assays were used to characterize the acetylation patterns of individual lysines under non-steady-state conditions. Sample preparation, including reaction quench, post-reaction propionylation, and tryptic digestion, were performed as in our previous published procedures [23, 33]. In order to reflect the fact that one Rtt109 molecule can only catalyze one molecular histone H3 at a time, as well as to easily compare the acetylation kinetic behavior with histone H3 alone, we use the H3/H4 dimer concentration to represent the concentrations of H3/H4, regardless of the conformation and complex.

Stoichiometry

We determined the recombinant *Xenopus* H3/H4 and Asf1 stoichiometry by titrating Asf1 and maintaining saturated H3/H4 and acetyl-CoA (25 and 300 μM , respectively) under steady-state conditions (0.3 μM Rtt109-Vps75). The H3/H4 and Asf1 mixture was prepared as described above and H3/H4 concentration was at least ten-fold higher than the dissociation constant (K_d) [15]. The apparent catalytic constant ($k_{\text{cat(app)}}$) was plotted as a function of the molar ratio of Asf1:H3/H4. Under these conditions, the protein ratio at which the $k_{\text{cat(app)}}$ reaches its plateau was determined to be the stoichiometry.

Sample analysis via UPLC-MS/MS

A Waters Acquity H-class UPLC (Milford, MA) coupled with a Thermo TSQ Quantum Access (Waltham, MA) triple quadrupole mass spectrometer (MS) was used to quantify the acetylated lysines on H3 and H4 peptides. The UPLC and MS/MS settings, solvent gradient, detailed mass transitions, and peak identification/quantification were reported in our previously published work [23, 24, 33]. Retention time and specific mass transitions were both used to identify individual acetylated and propionylated peaks. The resolved peak integration was done using Xcalibur software (version 2.1, Thermo). Relative quantitative analysis was used to determine the amount of acetylation on individual lysines [23, 33–35].

Data analysis

All the data were fit with Prism (version 5.0d). The initial rates (v) of acetylation were calculated from the linear increase in acetylation as a function of time prior to a total 10% acetylation. For individual lysines, the steady-state parameters $k_{cat(app)}$, $K_{(app)}$ (*i.e.* $K_{m(app)}$ or $K_{1/2(app)}$), and Hill coefficient (nH) were determined by fitting eq. 1, where $[S]$ is the concentration of substrate (H3, H3/H4, H3/H4-Asf1, or acetyl-CoA), and $[E]$ is the concentration of Rtt109-Vps75. In the case of multiple competitive sites with comparable acetylation rates and the same Hill coefficient, a one-site model is suitable to determine the specificity of each site, since the value of the specificity constant ($k_{cat(app)}/K_{m(app)}$ or $k_{cat(app)}/K_{1/2(app)}^{nH}$) is conserved for individual sites [23]. In addition, in cases where histones are not limiting, the $k_{cat(app)}$ is a viable measure for investigating the changes of enzyme specificity.

$$\frac{v}{[E]} = k_{cat(app)} \frac{[S]^{nH}}{([S]^{nH} + K_{(app)}^{nH})} \quad \text{eq.1}$$

To determine the second order rate constant (k_{nE}) for nonenzymatic acetylation under the conditions of excess acetyl-CoA, nonenzymatic acetylation was described by a single exponential equation (eq. 2), where $[P]_t$ is the concentration of a specific acetylated lysine at an individual sampling time point, t is the time, and k_{obs} is the observed rate.

$$[P]_t = [P]_{\infty} (1 - e^{-k_{obs}t}) \quad \text{eq.2}$$

The second order rate constant for nonenzymatic acetylation was determined by eq. 3, where k_{obs} is the pseudo-first order rate constant of acetylation from eq. 2, $[acCoA]$ is the concentration of acetyl-CoA, k_{nE} is the second order rate constant, and b is the y-intercept.

$$k_{obs} = k_{nE}[acCoA] + b \quad \text{eq.3}$$

The catalytic proficiency ($(k_{cat}/K_m)/k_{nE}$) was used to represent the ability of an enzyme to enhance acetylation. In addition, the $\Delta\Delta G$ for specific lysine residue was calculated using eq. 4, where R is the gas constant, T is the absolute temperature, (k_{cat}/K_m) is the specificity constant for the residue of interest, and k_{nE} is the second order rate constant for nonenzymatic acetylation. Using $\Delta\Delta G$, it is easier to recognize the enzyme preferences on different sites, because the specificity and selectivity could be quantified [23].

$$\Delta\Delta G = -RT \ln \left(\frac{k_{cat}/K_m}{k_{nE}} \right) \quad \text{eq.4}$$

Yeast histone extraction

The yeast histone purification is based on established protocols with minor modifications [36]. Briefly, yeast BY4741 (wt), *asf1Δ*, and *rtt109Δ* strains were cultured in YPD (1% yeast extract, 2% peptone and 2% glucose) and collected at OD600 of ~1.0 by centrifuging. The cell pellets were washed and incubated in DTT-Tris-HCl buffer at 30°C for 15 minutes. The cells were then digested with zymolyase at the final enzyme concentration of ~2 mg/ml for 60 to 90 minutes. After centrifugation pellets were resuspended in buffer, with the addition of H₂SO₄ to extract histones followed by TCA precipitation. The extracted yeast histones of these three strains were analyzed by UPLC-MS/MS.

Western blotting

Yeast cells were grown overnight in rich media, diluted and allowed to undergo 2 cell doublings. When cultures reached an OD600 of about 1.0, cells were harvested and lysed with 2 x SDS sample buffer. Proteins were denatured at 95°C for 5 minutes. Supernatants of total lysates were used for western blotting analysis. Approximately equal amount of total proteins were resolved by 15% SDS-PAGE followed by transferring of the proteins to a nitrocellulose membrane. Primary antibodies used in this study include polyclonal rabbit anti-Histone H3 (Abcam, Cambridge, MA), anti-acetylated H3K9 (Millipore), and anti-acetylated H3K23 (Millipore); each blot was also probed with polyclonal rabbit anti-TBP (as a reference). The secondary antibody was fluorescence labeled IR800 goat anti-rabbit (Rockland, Gilbertville, PA). The blots were visualized with an Odyssey infrared dual laser scanning unit (LI-COR Biotechnology, Lincoln, NE).

Results

Identification and quantification of Rtt109-Vps75-mediated acetylation on H3/H4

We have demonstrated that this multiplex targeted MS technique can detect and quantify the extent of individual acetylated lysine residues on histone H3/H4 from one sample injection [23, 24]. Herein, we determined the extent of acetylation on individual lysine residues by Rtt109-Vps75 to understand the site preference of Rtt109-Vps75 acetylation on H3/H4 (Fig. 1). Sites where we detect less than 5% acetylation are not shown. This plot shows that Rtt109-Vps75 preferentially acetylates H3K9 and H3K23, while K14, K27, and K56 on H3 have only modest acetylation. Although Rtt109-Vps75 cannot effectively acetylate the lysines on H4 compared to H3, H4K12 is the primary acetylation site on H4. These acetylation patterns are in agreement with previous studies [3–5].

Specificity of Rtt109-Vps75-mediated acetylation of H3

Rtt109-Vps75 is able to acetylate multiple lysine residues on histones; however, the factors regulating the preference/order of acetylation of individual lysines remain poorly understood. While there are many factors that may influence acetylation specificity, one of these factors, different histone configurations, may play an important role in cells. Tsubota *et al.* reported a k_{cat} of H3 acetylation by Rtt109-Vps75 of 0.21 sec⁻¹, which is faster than that they reported for H3/H4 [18]. We hypothesized that this could be due to the fact that the structure of H3 is more dynamic, allowing greater access to multiple residues, resulting in more residues being acetylated. To address this possibility, we utilized mass spectrometry-based assays to investigate the residue specificity of H3 acetylation by Rtt109-Vps75. We identified only two residues acetylated by Rtt109-Vps75 under steady-state conditions (where the total amount of acetylation is

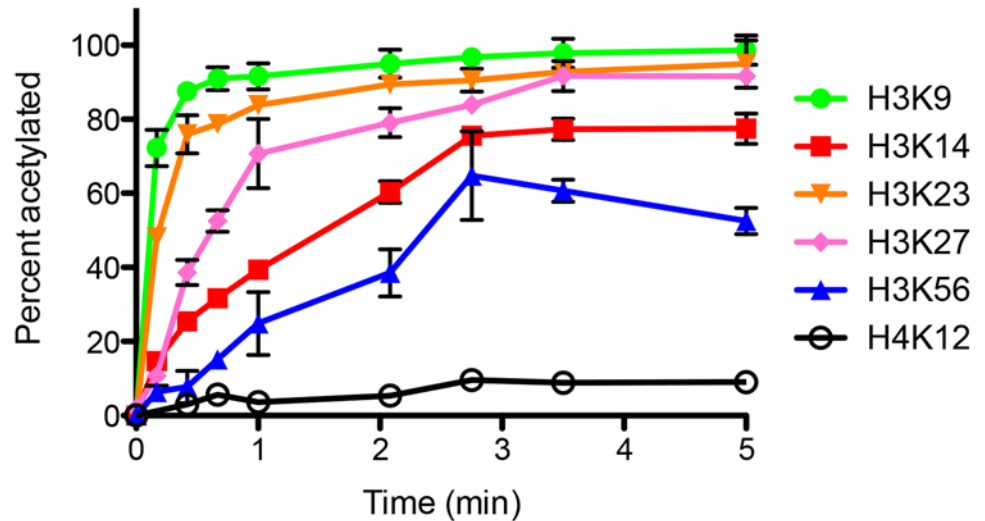


Fig 1. Time course study of acetylation on individual lysine residues of H3/H4 catalyzed by Rtt109-Vps75. The error bar indicates the standard error in acetylation percentage from three sets of assays. This assay indicates that H3K9 and H3K23 are the primary sites acetylated by Rtt109-Vps75, while H3K56 acetylation is modest.

doi:10.1371/journal.pone.0118516.g001

<10%); K9 and K23 (Fig. 2A and B). The specificity (k_{cat}/K_m) of Rtt109 for residues in H3 was the highest for K9, which is ~4-fold higher than K23 (Table 1).

Specificity of Rtt109-Vps75-mediated acetylation of H3/H4

Next we wanted to determine how the formation of tetramer would alter the specificity of Rtt109-Vps75 under saturating acetyl-CoA conditions. In these studies, we utilized H3 and H4 that was refolded into tetramer. However, all concentrations are listed as dimer concentrations instead of tetramer to make comparisons with data from H3 alone easier. With tetramer, we again only observed H3K9 and H3K23 acetylation under steady-state conditions. Under these conditions, the specificity for K9 was decreased by ~10-fold, and specificity for K23 was decreased by 2.5-fold when compared to H3 alone (Fig. 2C and D, Table 1). By comparing the specificity of Rtt109-Vps75 for one site to another, we obtained the selectivity of Rtt109-Vps75. We found that with the tetramer, there was no difference in selectivity between K9 and K23, which is not the case for H3 alone. Taken together, these data suggest that the order of specificity constants is $H3K9 > H3K23 > H3K9/H4 \cong H3K23/H4$ (Fig. 2A-D, Table 1).

Determining the stoichiometry of Asf1 to H3/H4 in Rtt109-Vps75 acetylation

Rtt109 is a unique KAT in that its activity is often linked to the presence of Vps75 and/or Asf1. However, the role of Asf1 in the Rtt109-mediated acetylation of H3 is not entirely clear. Several groups have suggested that Asf1 acts to alter the selectivity of Rtt109, resulting in the acetylation of H3K56 over other lysines [3–5, 14, 18]. It has been reported that Asf1 can stimulate acetylation for H3/H4 but not for H3 and that Asf1 will only form a complex with Rtt109 in the presence of H3/H4 [18]. While little work has been done utilizing both Vps75 and Asf1 together, the work that has been done suggests that they have an additive effect [14, 18]. While Vps75 interacts with the $(H3/H4)_2$ tetramer, Asf1 has been shown to split the $(H3/H4)_2$ tetramer into

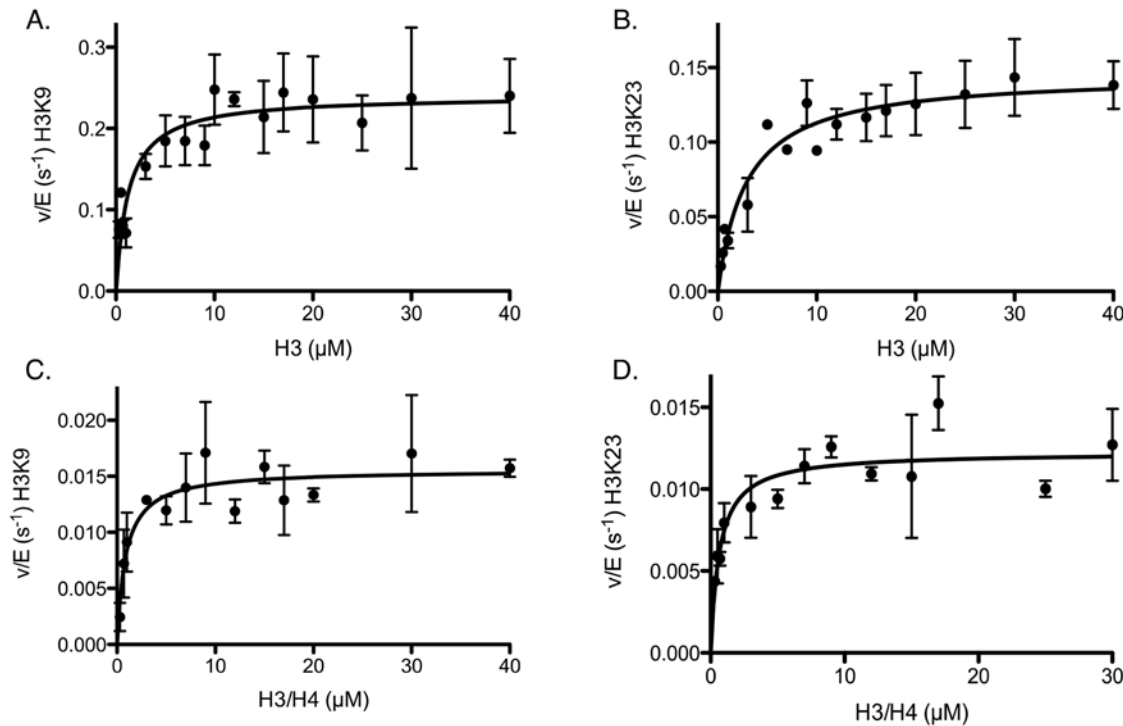


Fig 2. Determination of steady-state parameters for individual lysines of H3 and H3/H4 acetylation catalyzed by Rtt109-Vps75 when titrating histone in the presence of saturating acetyl-CoA. The detailed experimental conditions are described in the section “Steady-state kinetic assays for Rtt109-Vps75”. The error bar represents the standard error in v/E. Panels (A) and (B) show the Michaelis-Menten behaviors for H3K9 and H3K23, respectively, when titrating H3. Panels (C) and (D) also show the Michaelis-Menten behaviors for K9 and K23, respectively, when titrating H3/H4. H3 is the preferred substrate for Rtt109-Vps75 acetylation. The apparent kinetic parameters are summarized in Table 1.

doi:10.1371/journal.pone.0118516.g002

2(H3/H4) molecules, and has a tight affinity (of ~10 nM) [18, 21, 22, 37]. Given this available data, we hypothesize that H3/H4-Asf1 could be an ideal substrate for Rtt109-Vps75.

This hypothesis predicts that the optimal ratio of Asf1 to H3/H4 (dimer) would be 1:1 (or 1:0.5 for tetramer). To test this, we titrated Asf1 under conditions of saturating H3/H4 and acetyl-CoA (25 and 300 μM, respectively) and measured the changes of $k_{cat(app)}$ of Rtt109-Vps75. The concentration of H3/H4 was greater than the binding affinity of H3/H4 to Asf1 (13). Under these conditions, if the complex of Asf1 with H3/H4 (H3/H4-Asf1) acts as a substrate that facilitates Rtt109-Vps75 acetylation, we should see an approximately linear increase in acetylation rate as Asf1 is increased, reaching a plateau at a ratio of 1:1. However, if Asf1 is only acting to split (H3/H4)₂ to 2(H3/H4) without attaching to histones, we would observe maximal activation of Rtt109 acetylation at a concentration less than that of H3/H4, as Asf1 would not

Table 1. Steady-state parameters from kinetic assays of histone titration (mean ± standard error).

Substrate Titrated	Residue Acetylated	$K_{(app)}(\mu M)$	$k_{cat(app)}(x 10^{-2} s^{-1})$	$k_{cat}/K_m(x 10^{-2} \mu M^{-1} s^{-1})$
H3	H3K9	1.2 ± 0.3	24.0 ± 1.1	19.4 ± 5.2
H3	H3K23	2.9 ± 0.6	14.6 ± 0.7	5.0 ± 1.1
H3/H4	H3K9	0.9 ± 0.3	1.5 ± 0.07	1.8 ± 0.5
H3/H4	H3K23	0.6 ± 0.2	1.2 ± 0.06	1.9 ± 0.6
H3/H4-Asf1	H3K9	1.9 ± 0.5	6.2 ± 0.4	3.4 ± 1.0
H3/H4-Asf1	H3K23	2.1 ± 0.4	5.6 ± 0.3	2.6 ± 0.5

doi:10.1371/journal.pone.0118516.t001

have to remain bound to H3/H4 after splitting the tetramer. What we in fact observed was an increase in the rate of acetylation up to a ratio of 1 Asf1 to 1 H3/H4 ($K_9 = 1.21$ and $K_{23} = 1.09$) at which point the $k_{cat(app)}$ starts to level off (Fig. 3A and B). These data suggest that H3/H4-Asf1 acts as a substrate for Rtt109-Vps75.

H3/H4-Asf1 complex increases specificity but does not alter selectivity of Rtt109-Vps75

Once we determined that 1:1 Asf1 to H3/H4 dimer was the optimal ratio, we wanted to determine if Asf1 had any impact on the specificity/selectivity between residues. To our surprise, we observed no additional acetylated sites other than H3K9 and H3K23 in the presence of Asf1. However, we were still interested in determining the effects of Asf1 on the specificity of Rtt109-Vps75, so steady-state assays were conducted utilizing H3/H4-Asf1 as a substrate. Assays titrating H3/H4-Asf1 were performed in the presence of saturating acetyl-CoA. The H3/H4 concentrations were maintained at a level higher than the K_d of H3/H4 to Asf1 and a molar ratio of 1:1.2 (H3/H4:Asf1) to ensure that all H3/H4 is bound to Asf1. We observed negligible changes in selectivity (or preference) between K9 and K23 as compared to H3/H4 alone, but, based on changes in the $k_{cat(app)}$, we did see at least a 4-fold increase in specificity for both residues after the addition of Asf1 (Fig. 4A-D, Table 1). However, both the specificity constants and $k_{cat(app)}$ for H3/H4-Asf1 are still less than those for H3 alone (Table 1).

Acetyl-CoA has no impact on residue selectivity between H3K9 and H3K23 acetylation

It has been shown that acetyl-CoA concentration *in vivo* varies with different nutrient conditions, and that different acetyl-CoA concentrations could regulate histone acetylation [38–40]. Thus, after determining the different specificity on different histone substrates, we wanted to investigate if histone binding could have any impact on acetyl-CoA turnover, and whether the concentration of acetyl-CoA alters the selectivity between sites of acetylation, as it can with p300 and/or CBP [24].

To test this possibility, we performed a titration of acetyl-CoA with either saturating H3 or H3/H4, with the titrated concentrations of acetyl-CoA falling well within cellular acetyl-CoA concentrations [39]. When acetyl-CoA was titrated in the presence of H3, we no longer detected as large a difference in the specificity constants between K9 and K23 (Fig. 5A and B,

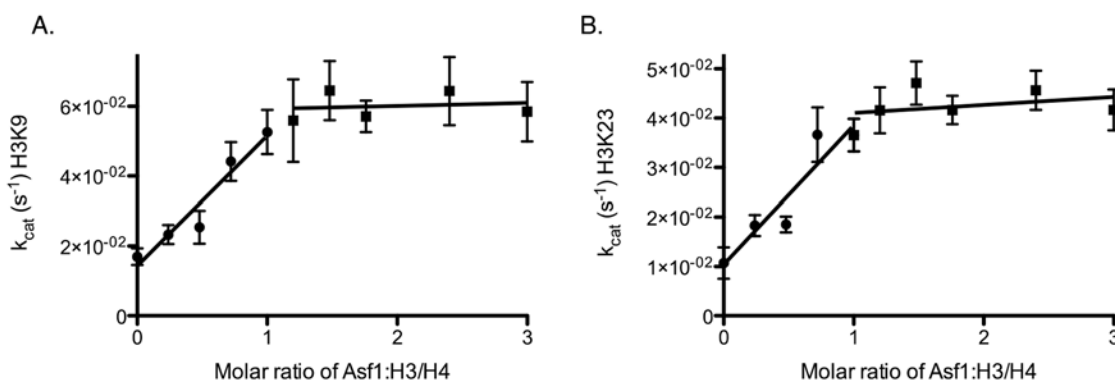


Fig 3. Stoichiometry of H3/H4-Asf1 for K9 and K23 in the presence of fixed concentrations of saturating acetyl-CoA and H3/H4. The detailed experimental conditions are described in the section “Stoichiometry”. The error bar represents the standard error in $k_{cat(app)}$. Panels (A) and (B) show that the acetylation rates of H3K9 and H3K23, respectively, increase as a function of molar ratio of Asf1 to H3/H4, before all H3/H4 binds with Asf1. The inflection points of H3K9 and H3K23 are 1.21 and 1.09, respectively, indicating that the binding stoichiometry of Asf1 and H3/H4 dimer is approximately 1:1.

doi:10.1371/journal.pone.0118516.g003

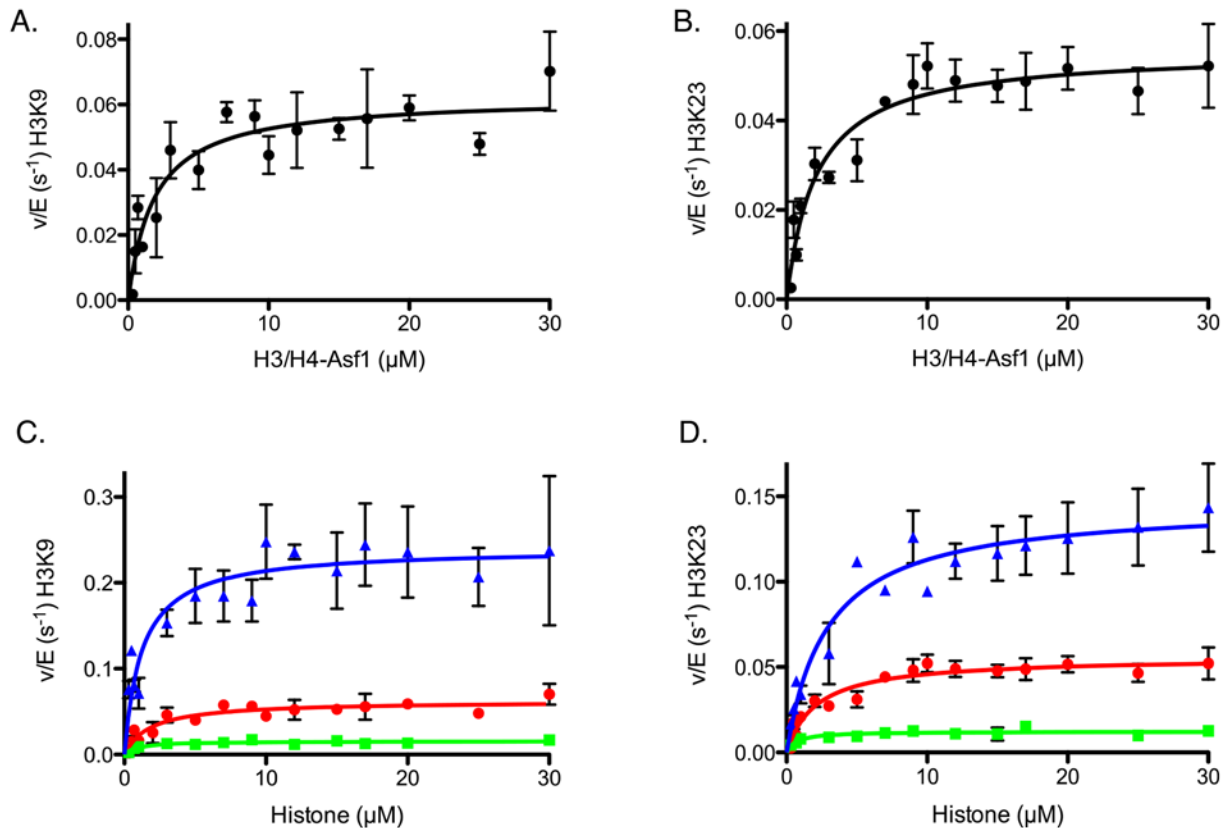


Fig 4. Determination of steady-state parameters of H3/H4-Asf1 acetylation catalyzed by Rtt109-Vps75 for individual lysines. The detailed experimental conditions are described in the section “Steady-state kinetic assays for Rtt109-Vps75”. The error bar represents the standard error in v/E. Panels (A) and (B) show the Michaelis-Menten behaviors for H3K9 and H3K23, respectively, when titrating H3/H4-Asf1 in the presence of saturating acetyl-CoA. Panels (C) and (D) show the superposition of steady-state kinetics for H3K9 and H3K23, respectively, on different histone conformations (H3: blue triangle, H3/H4-Asf1: red circle, and H3/H4: green square). The apparent kinetic parameters are summarized in Table 1. When H3/H4 is complexed with Asf1, no cooperativity is detected, and the specificity and selectivity of K9 and K23 acetylation increases.

doi:10.1371/journal.pone.0118516.g004

Table 2), which is mainly due to a similar K_m for both K9 and K23 when acetyl-CoA is limiting. For H3/H4, we did observe a sigmoidal or cooperative ($nH = 2$) dependence on acetyl-CoA for both K9 and K23 (Fig. 5C and D, Table 2). While the specificity of acetylation for H3/H4 decreased ~5-fold, the selectivity remained the same between the residues.

Finally, we sought to characterize whether the effect of acetyl-CoA on specificity is different in the presence on Asf1. As with the previous set of H3 and H3/H4 steady-state assays, we also performed acetyl-CoA titrations in the presence of saturating H3/H4-Asf1. Under saturating H3/H4-Asf1 conditions, we note that all of the titration plots from the steady-state assays of the H3/H4-Asf1 follow Michaelis-Menten kinetics (Fig. 5E and F). That indicates that there is no cooperativity when H3/H4-Asf1 is the histone substrate. Additionally, the specificity constants from the acetyl-CoA titrations were larger than those from the saturating H3/H4 condition but still smaller than those from saturating H3 alone (Table 2).

Nonenzymatic acetylation and catalytic proficiency of Rtt109-Vps75

We have previously characterized the nonenzymatic rate of acetylation for H3 [23]. The nonenzymatic rate of acetylation can be used to calculate the catalytic proficiency of each residue [23], and the difference between catalytic proficiency for different residues is a measurement of

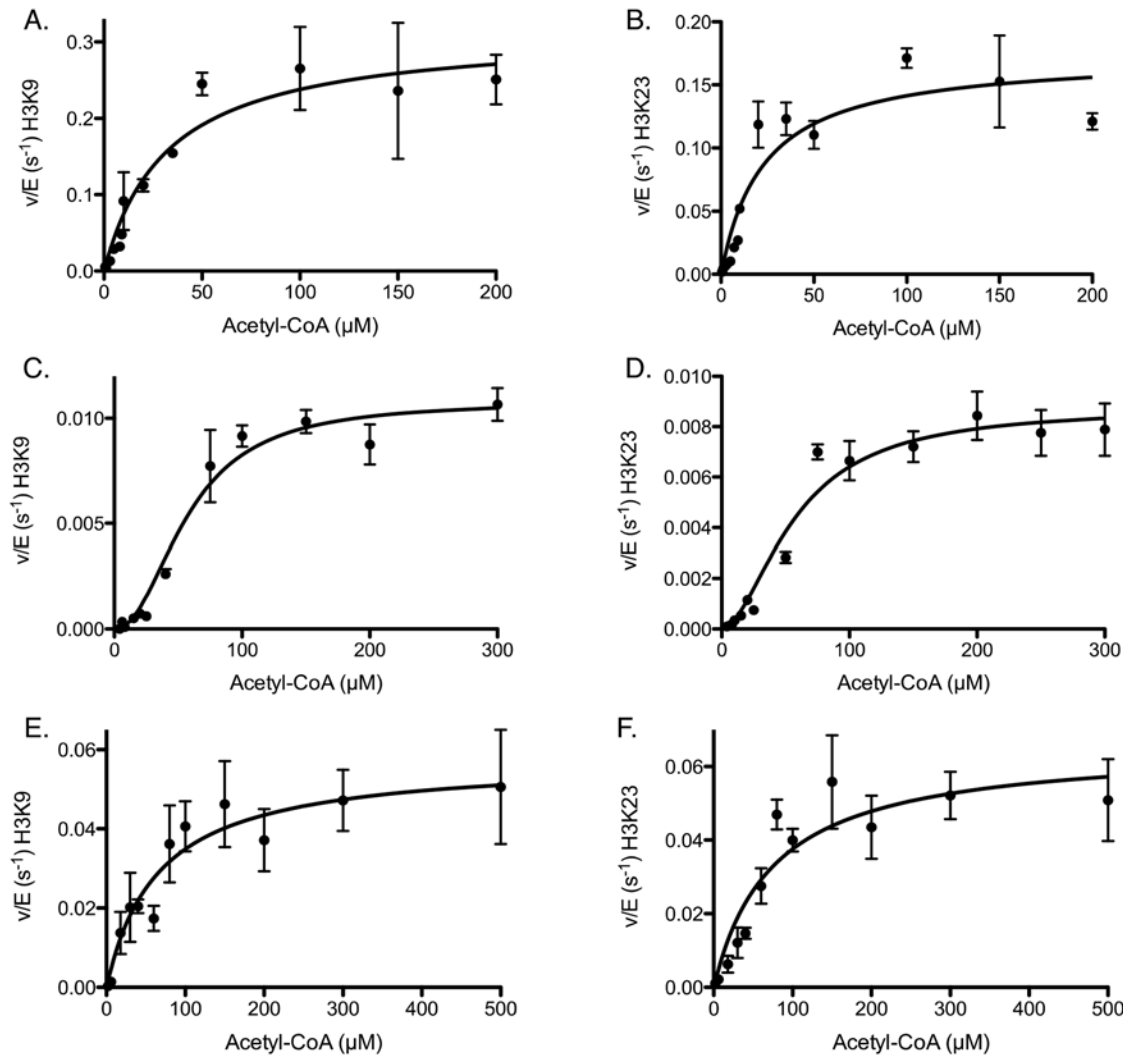


Fig 5. Determination of steady-state parameters for individual lysines of H3 and H3/H4 acetylation catalyzed by Rtt109-Vps75 when titrating acetyl-CoA in the presence of saturating histone. The detailed experimental conditions of the acetyl-CoA titration are described in the section “Steady-state kinetic assays for Rtt109-Vps75”. The error bar represents the standard error in v/E. Panels (A) and (B) show the Michaelis-Menten behaviors for H3K9 and H3K23, respectively. Panels (C) and (D) show the cooperativity for K9 and K23, respectively, for H3/H4. The Hill coefficient is approximately equal to 2, suggesting acetyl-CoA may have cooperative effects on the Rtt109-Vps75 (2:2) complex. Panels (E) and (F) show the Michaelis-Menten behaviors (no cooperativity) for K9 and K23, respectively, when titrating acetyl-CoA in the presence of saturating H3/H4-Asf1. The apparent kinetic parameters are summarized in Table 2.

doi:10.1371/journal.pone.0118516.g005

Table 2. Steady-state parameters from kinetic assays of acetyl-CoA titration (mean ± standard error).

Saturating Histone	Residue Acetylated	$K_{(app)}(\mu\text{M})$	nH	$k_{cat(app)}(\times 10^{-2} \text{ s}^{-1})$	$k_{cat}/K_m(\times 10^{-2} \mu\text{M}^{-1}\text{s}^{-1})$	$k_{cat}/K_{1/2}^{nH}(\times 10^{-6} \mu\text{M}^{-nH}\text{s}^{-1})$
H3	H3K9	32.4 ± 7.7	1	31.5 ± 2.6	0.9 ± 0.2	n.a.
H3	H3K23	23.0 ± 7.3	1	17.4 ± 1.8	0.7 ± 0.3	n.a.
H3/H4	H3K9	57.6 ± 5.9	2.1 ± 0.2	1.1 ± 0.05	0.018 ± 0.002	2.2 ± 0.1
H3/H4	H3K23	57.3 ± 7.2	1.8 ± 0.1	0.9 ± 0.04	0.015 ± 0.002	6.0 ± 0.3
H3/H4-Asf1	H3K9	65.7 ± 18.0	1	5.8 ± 0.5	0.09 ± 0.03	n.a.
H3/H4-Asf1	H3K23	75.2 ± 27.0	1	6.6 ± 0.8	0.09 ± 0.03	n.a.

doi:10.1371/journal.pone.0118516.t002

selectivity. From the results of nonenzymatic acetylation assays, there was no significant amount of acetylation detected on any of the lysines at the longest time point for steady-state assays (0.5 h). However, at longer incubation periods, we observed multiple acetylated lysines, including H3K9, H3K14, H3K18, H3K23, and H3K64. These data are consistent with previously reported data from our lab on residue selectivity of nonenzymatic acetylation, where nonenzymatic acetylation is not random but prefers H3K36 for H3 alone [23]. Under different buffer conditions (higher pH; see [Materials and Methods](#)), we found that H3K23 was the preferred site of acetylation for both H3 and H3/H4 for nonenzymatic acetylation. Although four other sites (H3K9, H3K14, H3K18, and H3K64) were also acetylated, due to the significantly slower rates we could not obtain the second order rate constants for these other sites.

Because H3K23 was the fastest nonenzymatic acetylation site, we defined the acetylation rate of H3K23 as the upper limit of nonenzymatic acetylation, and the k_{nE} were determined from H3K23 by [eq. 2](#) and [3](#) ($6.9 \pm 3.1 \times 10^{-8} \mu\text{M}^{-1}\text{s}^{-1}$ and $9.1 \pm 1.4 \times 10^{-8} \mu\text{M}^{-1}\text{s}^{-1}$ for H3 alone and H3/H4, respectively). These data suggest that buffer conditions (ionic strength and pH) have the largest effect on the selectivity of nonenzymatic acetylation relative to histone conformation.

We determined the selectivity between K9 and K23 by calculating the catalytic proficiency of the enzyme, $(k_{cat}/K_m)/k_{nE}$, and $\Delta\Delta G$ for residues K9 and K23 based on [eq. 4](#) (Tables [3](#) and [4](#)). The calculation of $(k_{cat}/K_m)/k_{nE}$ for H3/H4-Asf1 is based on the k_{nE} from H3/H4. For titrations of the histone, there was a 2.0×10^5 – 2.8×10^6 fold enhancement with Rtt109-Vps75 catalysis (Table [3](#)). This range accounts for the fact that different histone states or complexes resulted in different levels of catalytic enhancement. H3 demonstrates the highest catalytic enhancement of acetylation, H3/H4 the least and H3/H4-Asf1 is only slightly higher than H3/H4. Of the sites in H3, K9 was the preferred site catalyzed by Rtt109-Vps75, and there was no residue differences between K9 and K23 in either H3/H4 configuration.

For the acetyl-CoA titration, we observed a 1.7×10^3 – 2.4×10^5 fold acetylation enhancement by Rtt109-Vps75 (Table [4](#)). However, if the Hill coefficient is taken into account, the value of (k_{cat}/K_m) should be replaced by $(k_{cat}/K_{1/2}^{nH})$, and $\Delta\Delta G$ cannot be obtained from [eq. 4](#) (for details see [23]). A Hill coefficient of ~ 2 results in about a two-order of magnitude decrease in catalytic proficiency for the H3/H4 data but does not change the order of selectivity between the residues or affect which histone state is preferred as a substrate. In all conditions, H3 is the most catalytically proficient, and acetyl-CoA had no impact on the selectivity between H3K9 and H3K23.

In vivo loss of acetylation due to the loss of either Rtt109 or Asf1

Several labs have examined the loss of acetylation due to the loss of either Rtt109 or Asf1 [3, 4, 16, 25, 41], but the focus of these reports has largely been on the acetylation of H3K56. Western

Table 3. Catalytic proficiency of Rtt109-Vps75-mediated acetylation from histone titration (mean \pm standard error).

Histone Titrated	Residue Acetylated	$(k_{cat}/K_m)/k_{nE}$ (No unit)	$\Delta\Delta G$ (kcal/mol)
H3	H3K9	$(2.8 \pm 1.5) \times 10^6$	-9.1 ± 0.3
H3	H3K23	$(7.3 \pm 3.7) \times 10^5$	-8.3 ± 0.3
H3/H4	H3K9	$(2.0 \pm 0.7) \times 10^5$	-7.5 ± 0.2
H3/H4	H3K23	$(2.1 \pm 0.7) \times 10^5$	-7.5 ± 0.2
H3/H4-Asf1	H3K9	$(3.7 \pm 1.2) \times 10^5$	-7.9 ± 0.2
H3/H4-Asf1	H3K23	$(2.9 \pm 0.8) \times 10^5$	-7.7 ± 0.2

doi:10.1371/journal.pone.0118516.t003

Table 4. Catalytic proficiency of Rtt109-Vps75-mediated acetylation from acetyl-CoA titration (mean ± standard error).

Saturating Histone	Residue Acetylated	$(k_{cat}/K_m)/k_{NE}$ (No unit)	$(k_{cat}/K_{1/2}^{NH})/k_{NE}$ (μM^{-NH+1})	$\Delta\Delta G$ (kcal/mol)
H3	H3K9	$(1.4 \pm 0.7) \times 10^5$	n.a.	-7.3 ± 0.3
H3	H3K23	$(1.1 \pm 0.6) \times 10^5$	n.a.	-7.1 ± 0.4
H3/H4	H3K9	$(2.1 \pm 0.4) \times 10^3$	$(2.4 \pm 0.4) \times 10^1$	n.a.
H3/H4	H3K23	$(1.7 \pm 0.3) \times 10^3$	$(6.6 \pm 1.0) \times 10^1$	n.a.
H3/H4-Asf1	H3K9	$(9.7 \pm 3.2) \times 10^3$	n.a.	-5.6 ± 0.2
H3/H4-Asf1	H3K23	$(9.6 \pm 4.0) \times 10^3$	n.a.	-5.6 ± 0.3

doi:10.1371/journal.pone.0118516.t004

blots demonstrated a loss of H3K9 that is consistent with results from Berndsen *et al.* [3], but we have not detected a significant decrease in H3K23 acetylation (Fig. 6A). As it is difficult to rule out issues related to using antibodies (e.g. cross reactivity and epitope occlusion), we chose to use our targeted MS approach to monitor histone acetylation in these mutations. In the present study, we grew each strain in duplicate and preformed three individual sample injections from each sample. From our MS analysis, we observed at least a 5% decrease in acetylation of H3K9 with the loss of either Rtt109 or Asf1, while there are no significant changes of acetylation detected on H3K23 from these two mutants (Fig. 6B), which is consistent with our observations from western blot analysis. If we assume that in the cell H3 mainly exists in complex with H4, then these data suggest that Asf1 is needed for optimal H3K9 acetylation by Rtt109, both *in vitro* and *in vivo*.

The results of our analyses indicate that Rtt109 is one of the essential KATs for H3K9 acetylation but not for H3K23 acetylation *in vivo*. This finding could be due to the fact that H3K9 has been proposed to be acetylated by only Rtt109 and Gcn5 in yeast [4], while H3K23 is likely to be acetylated by multiple KATs. In addition, the deletion of Asf1 results in the same amount of K9 acetylation loss as the deletion of Rtt109, suggesting Asf1 is necessary for Rtt109 acetylation *in vivo*.

Factors influencing H3K56 acetylation by Rtt109-Vps75

Rtt109 was originally identified for its ability to support the acetylation of H3K56 [2, 42, 43], but our data indicate that this is not its primary or initial site of acetylation under our experimental conditions. We identified one possible difference: the use of histones purified from chicken erythrocytes [44]. We therefore wanted to determine if these different histone substrates combined with longer incubation time are key to facilitating H3K56 acetylation. Before utilizing histones from chicken erythrocytes, we used our label-free MS-based method to identify whether any residues were already acetylated, prior to acetylation by Rtt109-Vps75. We detected preexisting acetylation on histones from chicken erythrocytes of ~25% H3K14ac and ~12% H3K23ac, while there is no significant acetylation found on any other lysine residues of chicken erythrocyte histones. We also determined that no lysines from recombinant yeast nor *Xenopus* histones were acetylated prior to our experiments. Additionally, it is likely that other modifications exist on the chicken erythrocyte histones (such as methylation or phosphorylation) that we did not detect in this assay. Therefore, chicken histones present a complex background that is not suitable for kinetic studies. However, utilizing the chicken histones allows us to estimate the impact of pre-modified histones. Thus, we incubated 15 μM H3/H4 (recombinant yeast, *Xenopus* histones or histones purified from chicken erythrocytes) and 0.43 μM Rtt109-Vps75 (about the same level used for steady-state assays) for a longer time (1h). Under these conditions, we detected modest acetylation of K56, on both recombinant histones.

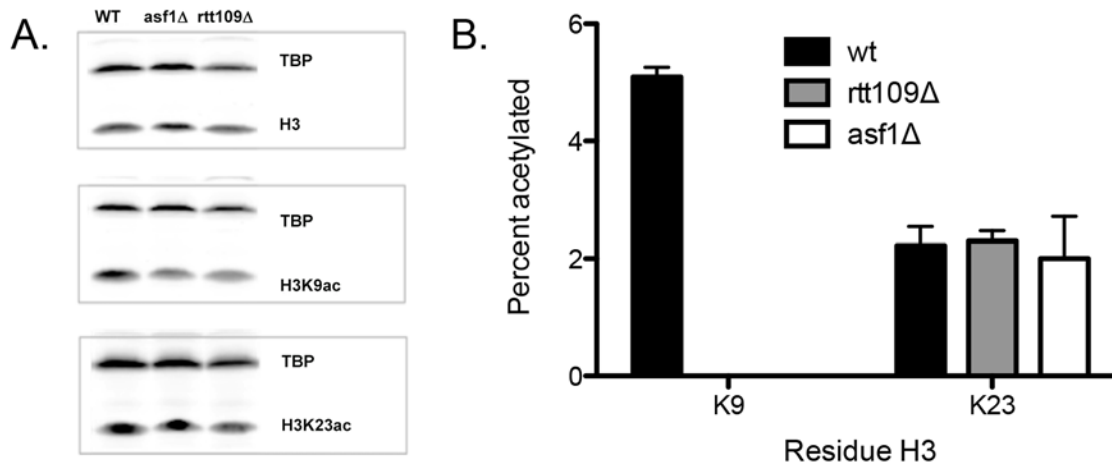


Fig 6. Changes *in vivo* due to the loss of either Rtt109 or Asf1. (A) Western blots using antibodies for H3, H3K9 or H3K23, using whole cell extracts from wild type (wt), *rtt109Δ*, and *asf1Δ* strains. (B) Determination of the percentage of acetylation at position H3K9 or H3K23 in wt, *rtt109Δ*, and *asf1Δ* strains using the targeted MS-based method. The error bar represents the standard error in acetylation percentage.

doi:10.1371/journal.pone.0118516.g006

However, the major site of acetylation on native chicken histone was H3K56 (Fig. 7). Although there were slight differences in the extent of acetylation between recombinant *Xenopus* and yeast histones, the preferences of Rtt109-Vps75 acetylation remained the same. The requirement for additional post-translational modification(s) presents a potential cause for this alteration in the specificity/selectivity of Rtt109-Vps75 towards K56 acetylation.

Discussion

Rtt109-Vps75 targets lysines on histones that are involved in genome stability and nucleosome assembly. In order to understand the extent to which Rtt109-Vps75 targets specific lysines in histone, we used a label-free quantitative MS-based assay to determine the specificity and selectivity of Rtt109-Vps75 on individual lysines of different histone substrates. In doing so, we have expanded our understanding of how chaperones help to facilitate Rtt109 dependent acetylation.

Much of the previously published work on Rtt109 has been done using classical techniques that either quantitate the total amount of acetylation or identify the locations of acetylation, but not both. Because of this limitation, the investigation of the specificity/selectivity of this enzyme is incomplete. Targeted MS can overcome this problem, allowing us to accurately measure the increases in catalytical activity and/or the changes in selectivity for individual sites.

We have previously shown with p300 that the histone configuration (H3 or H3/H4) can affect the specificity of a KAT. Here we observed that H3 was a much better substrate for Rtt109-Vps75 than H3/H4. We also observed a higher specificity for K9 and K23 on histone H3 alone, compared to H3/H4. Rtt109-Vps75 prefers K9 and K23 to other residues in all cases, with H3 being the preferred substrate *in vitro*. While *in vivo* a majority of H3 is bound to H4 to form either a histone-histone chaperone complex or a nucleosome, it cannot be ruled out that H3 is a possible substrate *in vivo*. Furthermore, the role of H3K9 acetylation in newly produced histones and their deposition in yeast [45], could suggest that Rtt109-Vps75 plays an important role in histone deposition of newly synthesized histone H3.

We observed no significant difference in selectivity between K9 and K23 on different histone configurations with decreasing acetyl-CoA, which suggests that reduced levels of acetyl-CoA in the cell will not affect the selectivity between these two primary sites acetylated by

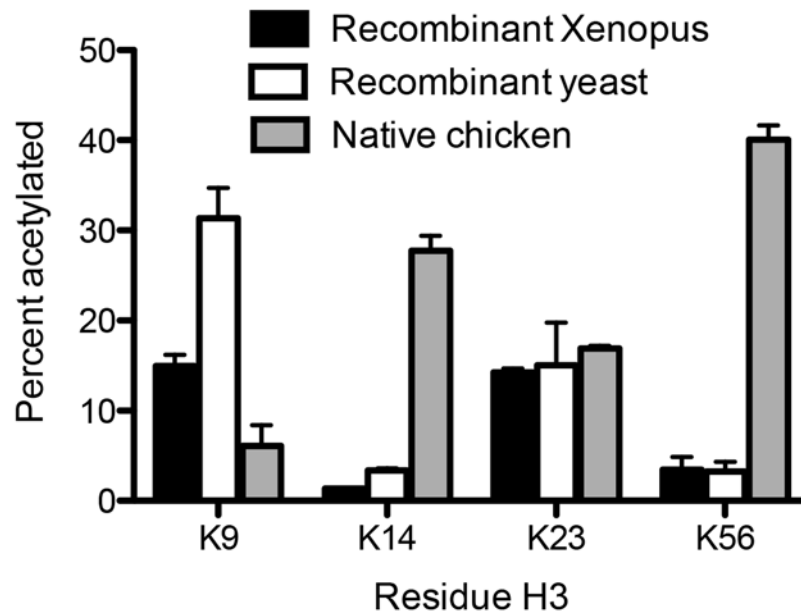


Fig 7. Comparison of Rtt109-Vps75 mediated acetylation (1-h incubation) on individual lysines on H3 from chicken erythrocytes, recombinant *Xenopus* histones, or recombinant yeast histones. Acetylation percentage of each site was determined by targeted MS-based method. The black and white bars depict the acetylation levels on recombinant *Xenopus* and yeast histones, respectively. The grey bar represents the acetylation levels on native chicken H3/H4 after 1 hour incubation with Rtt109-Vps75. The error bar represents the standard deviation in acetylation percentage from triplicate measurements. Note that the acetylation amount on both recombinant histones is initially negligible; however, there is ~25% H3K14ac and ~12% H3K23ac preexisting acetylation on chicken histones.

doi:10.1371/journal.pone.0118516.g007

Rtt109-Vps75. In addition, when titrating acetyl-CoA, the cooperativity ($nH = 2$) was only observed in the presence of saturating H3/H4, but not when titrating H3/H4 in saturating acetyl-CoA. One possible explanation for this could stem from the fact that the Rtt109-Vps75 complex is reported to be a 2:2 complex [15, 17]. It is also known that one acetyl-CoA binds to one Rtt109, which then allows Rtt109 to acetylate histones. At low levels of acetyl-CoA, it is more likely that only one of the two Rtt109 molecules in a complex with Vps75 dimer may have an acetyl-CoA molecule bound, and Vps75 dimer will bind one H3/H4 tetramer [15]. This will result in only one of the two H3 molecules being acetylated and thus the reduced acetylation efficiency. As the acetyl-CoA concentration increases, the probability of both Rtt109 molecules in complex having an acetyl-CoA molecule bound increases, and thus there is a non-hyperbolic increase in v/E as a function of acetyl-CoA. This model also explains why cooperativity is not observed in H3 monomer titrations.

In addition to Vps75, Asf1 has been suggested to alter the residues selectivity of Rtt109 [4, 5, 14, 18]. Asf1 interacts with H3/H4 dimer instead of $(H3/H4)_2$ tetramer [21, 22, 37]. In the present study, we followed up on the possibility that Asf1 binds H3/H4 dimer and functions as a substrate for Rtt109-Vps75. Tsubota *et. al.* reported that H3/H4 is required for interactions with Asf1 and increases the apparent acetylation rate of Rtt109-Vps75 [18]. Consistent with this finding, we observed a 1:1 stoichiometry of Asf1 to H3/H4 dimer and 4~5-fold increases in the $k_{cat(app)}$. Further supporting a model where H3/H4-Asf1 is acetylated by Rtt109-Vps75 is the fact that when we titrated acetyl-CoA under saturating H3/H4-Asf1, we lost the cooperativity observed in the H3/H4 alone reactions. Given the current structural model of 2:2 Rtt109:Vps75 and this loss of cooperativity, it suggests that H3/H4-Asf1

interaction with Rtt109-Vps75 increases the rate of acetylation. Therefore, Asf1 may enhance Rtt109-Vps75 activity by correctly positioning the histone substrate in the primed Rtt109 active site with acetyl-CoA.

While it has previously been demonstrated that the total acetylation of H3/H4 is enhanced by the introduction of Asf1 to Rtt109-Vps75 *in vitro* [14, 25], the analyses of each of the individual lysines have not been reported due to the aforementioned limitations of detection. Han and coworkers reported that H3K56 acetylation is enhanced by adding Asf1 into Rtt109-Vps75 and H3/H4 [14], and our data demonstrate that Asf1 enhances Rtt109-Vps75 acetylation on H3K9 and HK23 without altering the selectivity or preference between possible sites. This would mean that even if K56 acetylation has been increased, but is still a secondary site, we would not detect significant acetylation on K56 prior to 10% acetylation of the primary sites. We also conclude that an increase in specificity due to additional Asf1 is from a significant increase in $k_{\text{cat}(\text{app})}$ and to a lesser degree $K_{(\text{app})}$ (Tables 1 and 2). This finding is consistent with the study of Rtt109-Vps75 and H3/H4-Asf1 in which no significant enhancement in binding is observed [25], although it is unclear how the spatial arrangement of this H3/H4-Asf1 complex could influence the reaction rate. Thus, we suggest that Vps75 and Asf1 work together to promote histone acetylation in the cell. Consistent with this result, we observed the same amount of decrease in K9 acetylation *in vivo* with the loss of either Asf1 or Rtt109, suggesting that both are needed for proper acetylation.

Preexisting modification patterns are capable of altering the acetylation pattern of Rtt109-Vps75, as seen using histones extracted from chicken erythrocytes. Chicken erythrocyte histones were the only factor capable of altering the selectivity such that Rtt109-Vps75 preferentially acetylated H3K56. However, preexisting histone modifications unfortunately confound the results, because there is no one modification to which the altered selectivity can be attributed. Further evidence that preexisting modifications can alter selectivity is the fact that we observed suppression of K9 and K23 acetylation when utilizing chicken erythrocyte histones. This suggests that preexisting modifications on the histones have a bigger influence on residue selectivity than histone chaperones. While K56 acetylation is likely to occur secondarily to K9 and K23 acetylation no matter what the concentrations of Rtt109-Vps75 are, K56 acetylation may not be dependent on K9 and K23 acetylation, but instead is simply less favorable. This idea is supported by the fact that native chicken histones have modest H3K9 and H3K23 acetylation by Rtt109-Vps75 but significant enhancement of K56 acetylation (Fig. 7). However, under steady-state conditions using histones with no preexisting marks, Rtt109-Vps75 is not capable of acetylating K56 efficiently. In addition, we utilized either H3K9ac/H4 or H3K23ac/H4 tetramer as a starting substrate for 1-h incubation with Rtt109-Vps75 (same experimental condition of the assay for Fig. 7). After 1 hour, K56 of H3K9ac/H4 or H3K23ac/H4 tetramer were both ~3.9% acetylated, which is similar to the moderate acetylation of K56 detected from unmodified recombinant *Xenopus* and yeast histone tetramer ($3.4 \pm 1.4\%$ and $3.2 \pm 1.1\%$, respectively). Because of the high level of K56 acetylation detected when utilizing native chicken histones, these data suggest that some initial post-translational modification(s), but not K9 and K23 acetylation, alters the specificity and selectivity of Rtt109-Vps75 to favor K56 acetylation.

These data highlight that histone conformations (monomer, tetramer, and histone-chaperone complex) have significant effects on residue specificity for enzymatic acetylation. This suggests that chromatin dynamics play an important role in the specificity of KATs, linking both aspects of histone chaperones, which can both alter chromatin dynamics and histone conformation, which in turn influences acetylation. In this paper, we present evidence of increased specificity by two different chaperones interacting with different proteins: Rtt109-Vps75 and H3/H4-Asf1 working together for optimal acetylation. Finally, together these data demonstrate that a label-free quantitative mass spectrometry-based assay is a useful tool to

facilitate the understanding of enzyme kinetics, and provide a better understanding of protein-chaperone interactions and their role in histone acetylation.

Acknowledgments

We are grateful to Drs. Karolin Luger and Ronen Marmorstein for the generous gifts of purified recombinant *Xenopus* histone H3 and H4 and the plasmid of Rtt109-Vps75, respectively. We thank Dr. Artem Demidenko (Dr. Vasily Studitsky's lab) and Dr. Noah Wolfson (Dr. Carol Fierke's lab) offering H3/H4 tetramer purified from chicken erythrocytes and recombinant *Xenopus* H3K9ac/H4 and H3K23ac/H4 tetramers, respectively.

Author Contributions

Conceived and designed the experiments: YMK LAS AJA. Performed the experiments: YMK RAH LH XC. Analyzed the data: YMK LH AJA. Contributed reagents/materials/analysis tools: YMK. Wrote the paper: YMK RAH LAS AJA.

References

1. Tang Y, Holbert MA, Wurtele H, Meeth K, Rocha W, Gharib M, et al. Fungal Rtt109 histone acetyltransferase is an unexpected structural homolog of metazoan p300/CBP. *Nat Struct Mol Biol.* 2008; 15: 738–745. doi: [10.1038/nsmb.1448](https://doi.org/10.1038/nsmb.1448) PMID: [18568037](https://pubmed.ncbi.nlm.nih.gov/18568037/)
2. Schneider J, Bajwa P, Johnson FC, Bhaumik SR, Shilatifard A. Rtt109 Is required for proper H3K56 acetylation—A chromatin mark associated with the elongating RNA polymerase II. *J Biol Chem.* 2006; 281: 37270–37274. PMID: [17046836](https://pubmed.ncbi.nlm.nih.gov/17046836/)
3. Berndsen CE, Tsubota T, Lindner SE, Lee S, Holton JM, Kaufman PD, et al. Molecular functions of the histone acetyltransferase chaperone complex Rtt109-Vps75. *Nat Struct Mol Biol.* 2008; 15: 948–956. PMID: [19172748](https://pubmed.ncbi.nlm.nih.gov/19172748/)
4. Fillingham J, Recht J, Silva AC, Suter B, Emili A, Stagljar I, et al. Chaperone control of the activity and specificity of the histone H3 acetyltransferase Rtt109. *Mol Cell Biol.* 2008; 28: 4342–4353. doi: [10.1128/MCB.00182-08](https://doi.org/10.1128/MCB.00182-08) PMID: [18458063](https://pubmed.ncbi.nlm.nih.gov/18458063/)
5. Abshiru N, Ippersiel K, Tang Y, Yuan H, Marmorstein R, Verreault A, et al. Chaperone-mediated acetylation of histones by Rtt109 identified by quantitative proteomics. *J Proteomics.* 2013; 81: 80–90. doi: [10.1016/j.jprot.2012.09.026](https://doi.org/10.1016/j.jprot.2012.09.026) PMID: [23036725](https://pubmed.ncbi.nlm.nih.gov/23036725/)
6. Shimko JC, North JA, Bruns AN, Poirier MG, Ottesen JJ. Preparation of fully synthetic histone H3 reveals that acetyl-lysine 56 facilitates protein binding within nucleosomes. *J Mol Biol.* 2011; 408: 187–204. doi: [10.1016/j.jmb.2011.01.003](https://doi.org/10.1016/j.jmb.2011.01.003) PMID: [21310161](https://pubmed.ncbi.nlm.nih.gov/21310161/)
7. North JA, Shimko JC, Javaid S, Mooney AM, Shoffner MA, Rose SD, et al. Regulation of the nucleosome unwrapping rate controls DNA accessibility. *Nucleic Acids Res.* 2012; 40: 10215–10227. doi: [10.1093/nar/gks747](https://doi.org/10.1093/nar/gks747) PMID: [22965129](https://pubmed.ncbi.nlm.nih.gov/22965129/)
8. Tropberger P, Pott S, Keller C, Kamieniarz-Gdula K, Caron M, Richter F, et al. Regulation of transcription through acetylation of H3K122 on the lateral surface of the histone octamer. *Cell.* 2013; 152: 859–872. doi: [10.1016/j.cell.2013.01.032](https://doi.org/10.1016/j.cell.2013.01.032) PMID: [23415232](https://pubmed.ncbi.nlm.nih.gov/23415232/)
9. Masumoto H, Hawke D, Kobayashi R, Verreault A. A role for cell-cycle-regulated histone H3 lysine 56 acetylation in the DNA damage response. *Nature.* 2005; 436: 294–298. PMID: [16015338](https://pubmed.ncbi.nlm.nih.gov/16015338/)
10. Chen C-C, Carson JJ, Feser J, Tamburini B, Zabaronic S, Linger J, et al. Acetylated lysine 56 on histone H3 drives chromatin assembly after repair and signals for the completion of repair. *Cell.* 2008; 134: 231–243. doi: [10.1016/j.cell.2008.06.035](https://doi.org/10.1016/j.cell.2008.06.035) PMID: [18662539](https://pubmed.ncbi.nlm.nih.gov/18662539/)
11. Downs JA. Histone H3 K56 acetylation, chromatin assembly, and the DNA damage checkpoint. *DNA Repair.* 2008; 7: 2020–2024. doi: [10.1016/j.dnarep.2008.08.016](https://doi.org/10.1016/j.dnarep.2008.08.016) PMID: [18848648](https://pubmed.ncbi.nlm.nih.gov/18848648/)
12. Park Y-J, Luger K. Histone chaperones in nucleosome eviction and histone exchange. *Curr Opin Struct Biol.* 2008; 18: 282–289. doi: [10.1016/j.sbi.2008.04.003](https://doi.org/10.1016/j.sbi.2008.04.003) PMID: [18534842](https://pubmed.ncbi.nlm.nih.gov/18534842/)
13. Ransom M, Dennehey BK, Tyler JK. Chaperoning histones during DNA replication and repair. *Cell.* 2010; 140: 183–195. doi: [10.1016/j.cell.2010.01.004](https://doi.org/10.1016/j.cell.2010.01.004) PMID: [20141833](https://pubmed.ncbi.nlm.nih.gov/20141833/)
14. Han JH, Zhou H, Li ZH, Xu RM, Zhang ZG. Acetylation of lysine 56 of histone H3 catalyzed by Rtt109 and regulated by Asf1 is required for replisome integrity. *J Biol Chem.* 2007; 282: 28587–28596. PMID: [17690098](https://pubmed.ncbi.nlm.nih.gov/17690098/)

15. Park YJ, Sudhoff KB, Andrews AJ, Stargell LA, Uger K. Histone chaperone specificity in Rtt109 activation. *Nat Struct Mol Biol.* 2008; 15: 957–964. PMID: [19172749](#)
16. Kolonko EM, Albaugh BN, Lindner SE, Chen YY, Satyshur KA, Arnold KM, et al. Catalytic activation of histone acetyltransferase Rtt109 by a histone chaperone. *Proc Natl Acad Sci USA.* 2010; 107: 20275–20280. doi: [10.1073/pnas.1009860107](#) PMID: [21057107](#)
17. Tang Y, Holbert MA, Delgosaie N, Wurtele H, Guillemette B, Meeth K, et al. Structure of the Rtt109-AcCoA/Vps75 complex and implications for chaperone-mediated histone acetylation. *Structure.* 2011; 19: 221–231. doi: [10.1016/j.str.2010.12.012](#) PMID: [21256037](#)
18. Tsubota T, Berndsen CE, Erkmann JA, Smith CL, Yang LH, Freitas MA, et al. Histone H3-K56 acetylation is catalyzed by histone chaperone-dependent complexes. *Mol Cell.* 2007; 25: 703–712. PMID: [17320445](#)
19. Keck KM, Pemberton LF. Interaction with the histone chaperone Vps75 promotes nuclear localization and HAT activity of Rtt109 in vivo. *Traffic.* 2011; 12: 826–839. doi: [10.1111/j.1600-0854.2011.01202.x](#) PMID: [21463458](#)
20. Donham DC, Scorgie JK, Churchill ME. The activity of the histone chaperone yeast Asf1 in the assembly and disassembly of histone H3/H4–DNA complexes. *Nucleic Acids Res.* 2011; 39: 5449–5458. doi: [10.1093/nar/gkr097](#) PMID: [21447559](#)
21. English CM, Adkins MW, Carson JJ, Churchill MEA, Tyler JK. Structural basis for the histone chaperone activity of Asf1. *Cell.* 2006; 127: 495–508. PMID: [17081973](#)
22. English CM, Maluf NK, Triplet B, Churchill ME, Tyler JK. ASF1 binds to a heterodimer of histones H3 and H4: a two-step mechanism for the assembly of the H3-H4 heterotetramer on DNA. *Biochemistry.* 2005; 44: 13673–13682. PMID: [16229457](#)
23. Kuo Y-M, Andrews AJ. Quantitating the specificity and selectivity of Gcn5-mediated acetylation of histone H3. *PLOS ONE.* 2013; 8: e54896. doi: [10.1371/journal.pone.0054896](#) PMID: [23437046](#)
24. Henry RA, Kuo Y-M, Andrews AJ. Differences in specificity and selectivity between CBP and p300 acetylation of histone H3 and H3/H4. *Biochemistry.* 2013; 52: 5746–5759. doi: [10.1021/bi400684g](#) PMID: [23862699](#)
25. Pupaibool J, Kottom TJ, Bouchonville K, Limper AH. Characterization of the *Pneumocystis carinii* histone acetyltransferase chaperone proteins PcAsf1 and PcVps75. *Infect Immun.* 2013; 81: 2268–2275. doi: [10.1128/IAI.01173-12](#) PMID: [23569117](#)
26. Luger K, Rechsteiner TJ, Richmond TJ. Preparation of nucleosome core particle from recombinant histones. *Methods Enzymol.* 1999; 304: 3–19. PMID: [10372352](#)
27. Dyer PN, Edayathumangalam RS, White CL, Bao Y, Chakravarthy S, Muthurajan UM, et al. Reconstitution of nucleosome core particles from recombinant histones and DNA. *Methods Enzymol.* 2003; 375: 23–44.
28. Tang Y, Poustovoitov MV, Zhao K, Garfinkel M, Canutescu A, Dunbrack R, et al. Structure of a human ASF1a–HIRA complex and insights into specificity of histone chaperone complex assembly. *Nat Struct Mol Biol.* 2006; 13: 921–929. PMID: [16980972](#)
29. Tang Y, Meeth K, Jiang E, Luo C, Marmorstein R. Structure of Vps75 and implications for histone chaperone function. *Proc Natl Acad Sci USA.* 2008; 105: 12206–12211. doi: [10.1073/pnas.0802393105](#) PMID: [18723682](#)
30. Gill SC, Von Hippel PH. Calculation of protein extinction coefficients from amino acid sequence data. *Anal Biochem.* 1989; 182: 319–326. PMID: [2610349](#)
31. Luger K, Mäder AW, Richmond RK, Sargent DF, Richmond TJ. Crystal structure of the nucleosome core particle at 2.8 Å resolution. *Nature.* 1997; 389: 251–260. PMID: [9305837](#)
32. Albaugh BN, Kolonko EM, Denu JM. Kinetic mechanism of the Rtt109-Vps75 histone acetyltransferase-chaperone complex. *Biochemistry.* 2010; 49: 6375–6385. doi: [10.1021/bi100381y](#) PMID: [20560668](#)
33. Kuo Y-M, Henry RA, Andrews AJ. A quantitative multiplexed mass spectrometry assay for studying the kinetic of residue-specific histone acetylation. *Methods.* 2014; 70: 127–133. doi: [10.1016/j.ymeth.2014.08.003](#) PMID: [25123533](#)
34. Liu B, Lin Y, Darwanto A, Song X, Xu G, Zhang K. Identification and characterization of propionylation at histone H3 lysine 23 in mammalian cells. *J Biol Chem.* 2009; 284: 32288–32295. doi: [10.1074/jbc.M109.045856](#) PMID: [19801601](#)
35. Schneider TD, Arteaga-Salas JM, Mentele E, David R, Nicetto D, Imhof A, et al. Stage-specific histone modification profiles reveal global transitions in the *Xenopus* embryonic epigenome. *PLOS ONE.* 2011; 6: e22548. doi: [10.1371/journal.pone.0022548](#) PMID: [21814581](#)
36. Edmondson DG, Smith MM, Roth SY. Repression domain of the yeast global repressor Tup1 interacts directly with histones H3 and H4. *Genes Dev.* 1996; 10: 1247–1259. PMID: [8675011](#)

37. Bowman A, Ward R, Wiechens N, Singh V, El-Mkami H, Norman DG, et al. The histone chaperones Nap1 and Vps75 bind histones H3 and H4 in a tetrameric conformation. *Mol Cell*. 2011; 41: 398–408. doi: [10.1016/j.molcel.2011.01.025](https://doi.org/10.1016/j.molcel.2011.01.025) PMID: [21329878](https://pubmed.ncbi.nlm.nih.gov/21329878/)
38. Cai L, Tu B. On acetyl-CoA as a gauge of cellular metabolic state. *Cold Spring Harbor Symp Quant Biol*. 2011; 76: 195–202. doi: [10.1101/sqb.2011.76.010769](https://doi.org/10.1101/sqb.2011.76.010769) PMID: [21900151](https://pubmed.ncbi.nlm.nih.gov/21900151/)
39. Gilibili RR, Kandaswamy M, Sharma K, Giri S, Rajagopal S, Mullangi R. Development and validation of a highly sensitive LC-MS/MS method for simultaneous quantitation of acetyl-CoA and malonyl-CoA in animal tissues. *Biomed Chromatogr*. 2011; 25: 1352–1359. doi: [10.1002/bmc.1608](https://doi.org/10.1002/bmc.1608) PMID: [21381064](https://pubmed.ncbi.nlm.nih.gov/21381064/)
40. Galdieri L, Vancura A. Acetyl-CoA carboxylase regulates global histone acetylation. *J Biol Chem*. 2012; 287: 23865–23876. doi: [10.1074/jbc.M112.380519](https://doi.org/10.1074/jbc.M112.380519) PMID: [22580297](https://pubmed.ncbi.nlm.nih.gov/22580297/)
41. Han JH, Zhou H, Li ZZ, Xu RM, Zhang ZG. The Rtt109-Vps75 histone acetyltransferase complex acetylates non-nucleosomal histone H3. *J Biol Chem*. 2007; 282: 14158–14164. PMID: [17369253](https://pubmed.ncbi.nlm.nih.gov/17369253/)
42. Driscoll R, Hudson A, Jackson SP. Yeast Rtt109 promotes genome stability by acetylating histone H3 on lysine 56. *Science*. 2007; 315: 649–652. PMID: [17272722](https://pubmed.ncbi.nlm.nih.gov/17272722/)
43. Lin CQ, Yuan YA. Structural insights into histone H3 lysine 56 acetylation by Rtt109. *Structure*. 2008; 16: 1503–1510. doi: [10.1016/j.str.2008.07.006](https://doi.org/10.1016/j.str.2008.07.006) PMID: [18707894](https://pubmed.ncbi.nlm.nih.gov/18707894/)
44. Radovani E, Cadorin M, Shams T, El-Rass S, Karsou AR, Kim H-S, et al. The Carboxyl terminus of Rtt109 functions in chaperone control of histone acetylation. *Eukaryot Cell*. 2013; 12: 654–664. doi: [10.1128/EC.00291-12](https://doi.org/10.1128/EC.00291-12) PMID: [23457193](https://pubmed.ncbi.nlm.nih.gov/23457193/)
45. Kuo M-H, Brownell JE, Sobel RE, Ranalli TA, Cook RG, Edmondson DG, et al. Transcription-linked acetylation by Gcn5p of histones H3 and H4 at specific lysines. *Nature*. 1996; 383: 269–272. PMID: [8805705](https://pubmed.ncbi.nlm.nih.gov/8805705/)